

Fundamental Aerodynamic Characteristics of Delta Wings with Leading-Edge Vortex Flows

Richard M. Wood* and David S. Miller*
NASA Langley Research Center, Hampton, Virginia

An investigation of the aerodynamics of sharp leading-edge delta wings at supersonic speeds has been conducted. The supporting experimental data for this investigation were taken from published force, pressure, and flow-visualization data in which the Mach number normal to the wing leading edge is always less than 1.0. The individual upper- and lower-surface nonlinear characteristics for uncambered delta wings are determined and presented in three charts. The upper-surface data show that both the normal-force coefficient and minimum pressure coefficient increase nonlinearly with a decreasing slope with increasing angle of attack. The lower-surface normal-force coefficient was shown to be independent of Mach number and to increase nonlinearly, with an increasing slope, with increasing angle of attack. These charts are then used to define a wing-design space for sharp leading-edge delta wings.

Nomenclature

\mathcal{R}	= aspect ratio
C_L	= lift coefficient
ΔC_L	= nonlinear incremental change in lift coefficient with respect to the linear lift coefficient = $C_{L\alpha=20 \text{ deg}} - (20) C_{L\alpha}$
$C_{L\alpha}$	= lift-curve slope
C_N	= normal-force coefficient
C_N^l, C_N^u	= wing lower- and upper-surface normal-force coefficients, respectively
ΔC_N	= nonlinear incremental change in normal-force coefficient with respect to the linear normal-force coefficient
C_p	= pressure coefficient
$C_{p,\min}^u$	= minimum wing upper-surface pressure coefficient
$C_{p,v}$	= vacuum pressure coefficient, = $-2/\gamma M^2$
ℓ	= configuration length
M	= Mach number
M_N	= component of Mach number normal to wing leading edge, = $M \cos \Lambda_{LE} (1 + \sin^2 \alpha \tan^2 \Lambda_{LE})^{1/2}$
S_N	= Reynolds number
x, y, z	= Cartesian coordinates
α	= angle of attack
α_N	= angle of attack normal to wing leading edge, = $\tan^{-1}(\tan \alpha / \cos \Lambda_{LE})$
β	= $\sqrt{M^2 - 1}$
η	= fraction of local wing semispan
Λ_{LE}	= wing leading-edge sweep angle

Introduction

AERODYNAMICISTS have pursued the goal of efficient supersonic flight for some time. Associated with supersonic flight are "real-flow" characteristics (compressibility,¹ vacuum limit,² and boundary-layer stability¹) which can significantly affect wing performance. For low levels of lift, the effect of these restrictive real-flow characteristics on aerodynamic performance has been identified and has

resulted in the development of the existing attached-flow, linear-theory-based, wing-design methods.^{3,4} Attached-flow wing-design methods have successfully produced optimum twisted and cambered wings for efficient low-lift supersonic flight at Mach numbers of 1.8-2.8.^{5,6} At high-lift conditions, the impact of compressibility, vacuum limit, and boundary-layer stability on wing design becomes more restrictive and the application of attached-flow wing-design methodology might prove unsuccessful. In general, linear-theory methods cannot accurately model the nonlinear characteristics which can dominate the lifting characteristics at these conditions, and nonlinear attached-flow wing-camber designs⁷ are susceptible to boundary-layer separation. An alternate high-lift wing-design concept that might not be as susceptible to boundary-layer separation would employ wing-leading-edge vortex flow. This separated-flow wing design approach would employ a leading-edge vortex that would be positioned on the forward portion, upper surface of a cambered wing where the vortex-induced suction pressures would produce both an increase in lift and a decrease in drag. The separated-flow wing-design philosophy has been studied extensively at subsonic speeds^{8,9} and has led to the design of several unique leading-edge devices,^{10,11} such as "vortex flaps." However, no significant amount of theoretical or experimental work has been conducted on the application of the separated-flow design philosophy at supersonic speed.

This paper discusses the real-flow limitations associated with wing leading-edge vortex flows for high-lift wing design at supersonic speeds, and identifies a wing-design space applicable for separated flows at supersonic speeds. The supporting information for this study was taken from published force, pressure, and flow-visualization data for flat and cambered delta wings.¹²⁻³⁴ All data presented in this paper are for conditions in which the Mach number normal to the leading edge is always less than 1.0.

Discussion

Background

Over the past 40 years, the understanding of wing leading-edge separated flows at supersonic speeds has not been pursued, theoretically or experimentally, with the same vigor as that for attached flows. The reasons for the lack of parallel growth between the two wing-design concepts are many. The two major contributors are probably the theoretical complexity involved in modeling separated flows and the belief that separated flows at supersonic speeds will always produce large

Presented, in part, as Paper 84-2208 at the AIAA 2nd Applied Aerodynamics Conf., Seattle, Wash., Aug. 21-23, 1984; received Aug. 31, 1984; revision received March 15, 1985. This paper is declared a work of the U.S. Government and therefore is in the public domain.

*Aero-Space Technologist, Fundamental Aerodynamics Branch, High-Speed Aerodynamics Division. Member AIAA.

drag penalties. An examination of the existing data base for sharp leading-edge delta wings raises some doubts about the validity of this second assumption for high-lift conditions. The data suggest that significant improvements in aerodynamic performance can be obtained through the management of wing leading-edge vortices.^{35,36}

The lifting characteristics of delta wings with subsonic, sharp leading edges at supersonic speeds have been documented extensively. In 1948, Mayer² identified the minimum attainable upper-surface pressure coefficient value to be 70% of the vacuum pressure coefficient. The identification of this upper-surface pressure limit has had a significant impact on supersonic wing camber design to the present day. In 1957, Hill¹³ presented the positive nonlinear increment in normal-force coefficient as a function of the parameter $\beta \cot \Lambda_{LE}$ (upper left of Fig. 1). The data indicate that for small values of $\beta \cot \Lambda_{LE}$, large increments in nonlinear normal force exist which could result in nonlinear lift. The combination of low Mach number and high leading-edge sweep conditions at which nonlinear lift occurs was supported further by the findings of Brown and Michael³⁷ in 1954 and Squire et al.^{27,35,38} in 1963, 1967, and 1980. The variation in nonlinear lift at supersonic speeds for delta wings at 20 deg angle of attack is presented as a function on the parameter $R\beta \cot \Lambda_{LE}$ in the upper right of Fig. 1. The figure shows that significant amounts of nonlinear increasing lift ($\Delta C_L > 0$) can be obtained for values of $R\beta \cot \Lambda_{LE}$ less than 0.50. For values of $R\beta \cot \Lambda_{LE}$ between 0.50 and 1.00, which has been the range of M and Λ_{LE} of primary interest for supersonic flight, nonlinear lift effects are not present. And for values of $R\beta \cot \Lambda_{LE}$ greater than 1.00, nonlinear decreasing lift ($\Delta C_L < 0$) occurs.

Another interesting correlation was performed by Love³¹ in 1955 in which the ratio of the experimental and theoretical lift-curve slope was presented as a function of the parameter $\beta \cot \Lambda_{LE}$ (lower left of Fig. 1). The figure shows that for values of $\beta \cot \Lambda_{LE}$ greater than 0.50, the experimental values of lift-curve slope never reach the level predicted by linear

theory and, for values of $\beta \cot \Lambda_{LE}$ between 0.50 and 1.00, there is essentially no increase in the experimental lift-curve slope. These results suggest that separated-flow wing designs should be performed for $\beta \cot \Lambda_{LE}$ between 0.50 and 0.70 to provide the maximum opportunity for vortex formation without a loss in lifting effectiveness.

In 1983, Miller and Wood³⁹ expanded on the Stanbrook-Squire boundary⁴⁰ by identifying six distinct attached- and separated-flow categories (bottom right of Fig. 1) for delta wings at angle of attack. Based upon the reclassification of the flow categories for delta wings, it was suggested that future supersonic separated-flow wing-design work should be performed for M_N less than 0.9 and α_N from 10 to 40 deg (shaded region). Within this range of normal angle of attack and normal Mach number, the data of Ref. 39 indicate that a wing leading-edge vortex will form and that a significant amount of vortex-induced suction force will be available for drag minimization.

Aerodynamics of Uncambered Delta Wings

To define a high-lift, separated-flow wing-design procedure, an understanding of the aerodynamic restrictions that exist at supersonic speeds is required. A review of the literature revealed a large amount of experimental force, pressure, and flow-visualization data for flat delta wings and a limited amount of similar data for cambered delta wings at supersonic speeds. This section of the paper will investigate how wing leading-edge sweep, Mach number, and angle of attack affects the lifting characteristics of the upper and lower wing surfaces of delta wings and will provide insight into their impact on the design of a separated-flow high-lift wing.

Through the compilation and correlation of the force and pressure data, the separated-flow aerodynamic characteristics and a separated-flow design space will be identified. By limiting this discussion to separated flows, the available design space shown in the bottom right of Fig. 1 can be reduced in half with the application of the attached-flow/separated-flow boundary (Fig. 3). The area below the boundary includes all three regions of separated-flow identified by Miller and Wood.³⁹

Further reductions in the size of the design space can be made with the identification of upper and lower Mach numbers of the supersonic envelope. For this discussion, the lower supersonic Mach number is defined as that value at which the leeside flow characteristics over a flat delta wing depart from a conical flow condition, and the upper Mach number for each wing leading-edge sweep initially will be identified by the attached/separated-flow boundary shown in Fig. 2. The lower Mach number boundary was identified to be $M = 1.2$ by reviewing pressure data for a series of delta wings at Mach numbers from 0.6 to 3.5.^{17,29} This lower Mach number boundary is shown in Fig. 3. An example of the data used to establish this lower Mach number boundary is presented in Fig. 4 as spanwise pressure distributions at different longitudinal (x/l) stations for an aspect ratio (R) 1.0 delta wing at Mach numbers of 0.6, 0.9, 1.2, and 1.6. The pressure data clearly show that nonconical flow conditions exist at both $M = 0.6$ and 0.9. However, between $M = 0.9$ and 1.2 the pressure data show a definite change from a nonconical nature to a very nearly conical flow on both the upper and lower surfaces. At a Mach number of 1.6, the spanwise pressure distributions are definitely conical and remain conical out to $M = 3.5$. Based upon this analysis, the lower supersonic Mach number was defined as 1.20.

Typical effects of Mach number and angle of attack on the spanwise pressure distribution for an $R = 1.0$ delta wing are presented in Fig. 5. From the data on the left of the figure, it can be shown that at a constant angle of attack of 15 deg, increasing the Mach number from 0.6 to 0.9, from 0.6 to 1.2, or from 0.6 to 1.6 results in a reduction in upper-surface normal-force coefficient (assuming conical flow) of 11, 34, and 43%, respectively. A reversal of these upper surface ef-

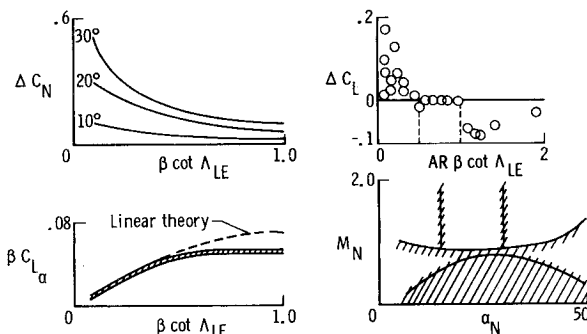


Fig. 1 Summary of flat delta wing aerodynamics.

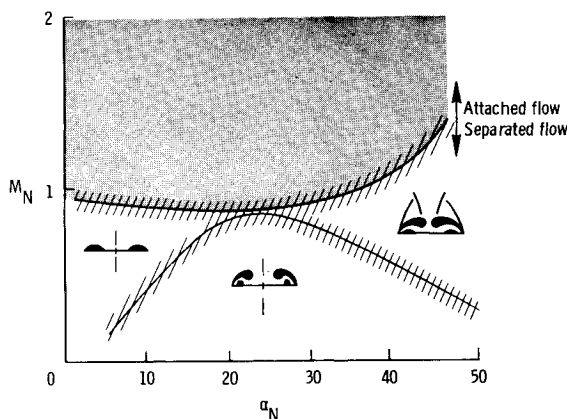


Fig. 2 Wing-design space upper boundary.

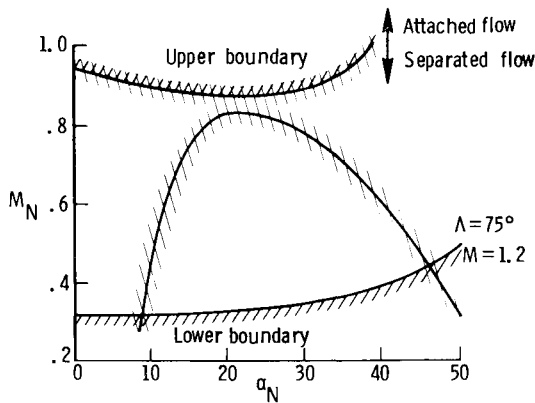
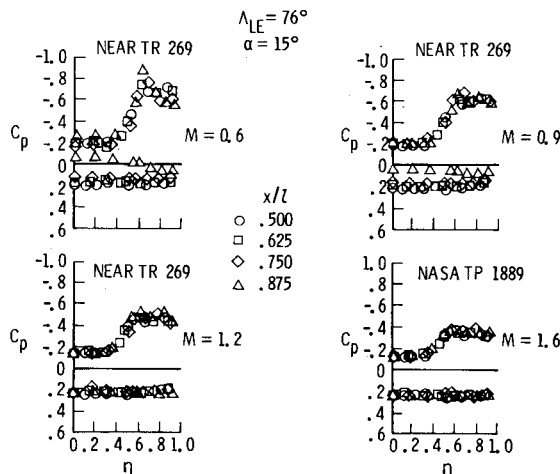
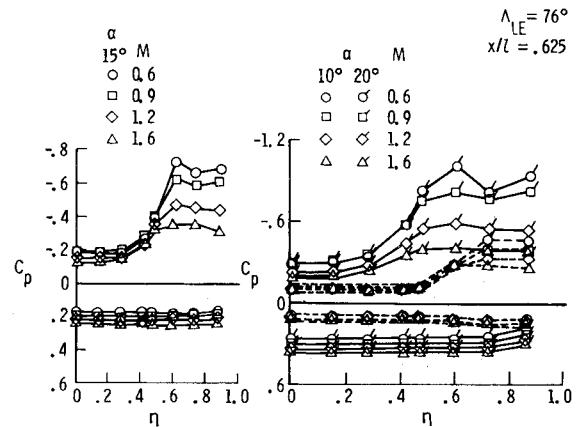


Fig. 3 Wing-design space lower boundary.

Fig. 4 Spanwise pressure distributions for an $R=1.0$ delta wing at $\alpha = 15$ deg.

fects is found on the lower surface where the lifting force increases (assuming conical flow) with an increase in Mach number. As Mach number increases, the gain in lower-surface lift does not completely compensate for the loss in upper-surface lift and the result is a loss in total lift coefficient with increasing Mach number at a constant angle of attack. The combination of a loss in the upper-surface lift with an increase in lower-surface lift highlights the impact of compressibility and vacuum limit on the lifting efficiency at supersonic speeds.

Presented on the right of Fig. 5 is the effect of increasing angle of attack on the spanwise pressure distribution at $M=0.6, 0.9, 1.2$, and 1.6 for the $R=1.0$ delta wing. The pressure data show that at $M=0.6$ and 0.9 , both the upper- and lower-surface pressures increase proportionately. The data for $M=1.2$ and 1.6 indicate a shift in lifting force from the upper to the lower surface. This effect is quantified in Fig. 6, which depicts the percentage of lift on both the upper and lower surfaces for both 10 and 20 deg angle of attack. The graph in Fig. 6 shows that at subsonic speeds ($M=0.6$ and 0.9), approximately 70% of the given lift (assuming conical flow) comes from the upper surface, regardless of angle of attack. At $M=1.2$ and $\alpha=10$ deg, the upper surface carries 70% of the lift, but at $\alpha=20$ deg this is reduced to 60%. This trend is even more pronounced at $M=1.60$ where at $\alpha=10$ deg the upper surface dominates with 65% of the lift, and at $\alpha=20$ deg it has been reduced to 40% of the lift. The shifting of lift from the upper to the lower surface with increasing angle of attack at supersonic speeds is a combination of nonlinearly decreasing upper-surface normal force (vacuum limit dominated effect) and nonlinearly increasing lower-surface

Fig. 5 Effect of Mach number and angle of attack on the spanwise pressure distributions at $x/l=0.625$ for $R=1.0$ delta wing.

normal force (compressibility dominated effect). These results suggest that only at subsonic speeds ($M<0.9$) can the lift increment between the linear potential-theory solution and experimental data belong solely to upper-surface vortex-induced effects. At both transonic and supersonic speeds, the lift increment is probably due to a combination of both nonlinear lower surface (compression) and nonlinear upper surface (vortex) effects. In particular, at supersonic speeds, the upper-surface vortex-induced lift increment reduces with increasing angle of attack and the lower-surface compression lift increment increases with increasing angle of attack.

A summary of the individual normal-force characteristics of the upper and lower surfaces for flat sharp leading-edge delta wings is presented in Figs. 7-9. Figures 7 and 9 were formulated by integrating experimental spanwise pressure distributions to extract a section upper- and lower-surface normal-force coefficient. The normal-force coefficients then were used to represent the wing upper or lower-surface normal-force coefficient based upon the known existence of conical flow for delta wings at supersonic speeds. The curves of Figs. 7-9 comprise a range of Mach number from 1.5 to 3.5 and leading-edge sweep of 58-85 deg. The results could not be produced for Mach numbers below 1.5 because of insufficient experimental data. As shown in Fig. 7, when the upper-surface normal-force coefficient ($C_p^{u,min}$) plotted as a function of the parameter $\alpha_N \beta \cot \Lambda_{LE}$, the data reduce to a family of constant Mach number curves. The large effect of Mach number on upper-surface normal force is clearly shown; for example, an increase in Mach number from 1.5 to 2.0 reduces the maximum upper-surface lifting potential by 50%. The large reduction in upper-surface lifting capability with increasing Mach number is due to the restriction of the upper-surface suction pressures by the vacuum pressure limit. The characteristics of the curves of Fig. 7 also indicate that for a given Mach number and leading-edge sweep, an increase in angle of attack will result in an upper-surface normal-force coefficient that increases nonlinearly with a decreasing slope. The data can be extrapolated (dashed line) to show that the upper-surface normal-force coefficient eventually will reach a maximum level and remain constant for all further increases in angle of attack.

Presented in Fig. 8 is the upper-surface minimum pressure coefficient ($C_p^{u,min}$) plotted as a function of the parameter $\alpha_N \beta \cot \Lambda_{LE}$. These data also form a family of constant Mach number curves. Also noted on this figure is the percent of vacuum limit which was attained for that particular Mach number. The data show that the percent of the vacuum pressure actually attained is reduced with increasing Mach number. At a Mach number of 3.50, only 75% of the vacuum limit was reached, however, at a Mach number of 1.50, 97% of the vacuum limit was attained. For Mach numbers below

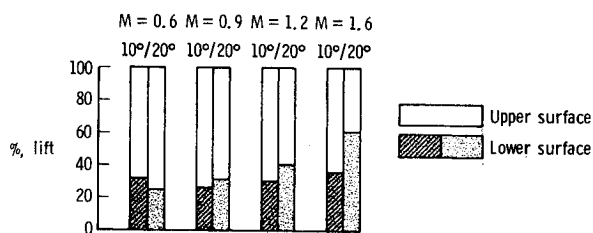


Fig. 6 Effect of Mach number and angle of attack on the distribution of lift between the upper and lower surface of an $AR = 1.0$ delta wing.

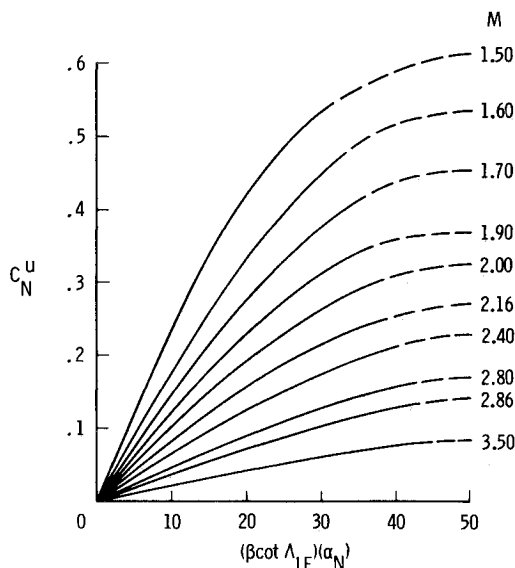


Fig. 7 Effect of Mach number, angle of attack, and leading-edge sweep on the upper-surface normal-force coefficient for flat delta wings.

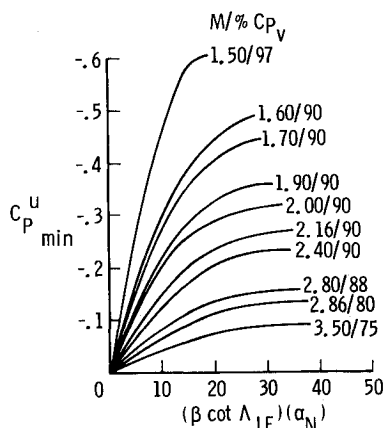


Fig. 8 Effect of Mach number, angle of attack, and leading-edge sweep on the upper-surface minimum pressure coefficient for flat delta wings.

1.50, the data suggest that 100% of the vacuum limit might be achievable. These results contradict the findings of Ref. 2 and indicate that the 70%-of-vacuum pressure limit is not generally applicable for the separated-flow, high-lift, wing-design concept.

The variation in the lower-surface normal-force coefficient is presented in Fig. 9. Unlike the data of Figs. 7 and 8, which showed that the upper-surface characteristics are a function of leading-edge sweep, Mach number, and angle of attack, the lower-surface characteristics were found to be only a function of leading-edge sweep and angle of attack. The lower-surface

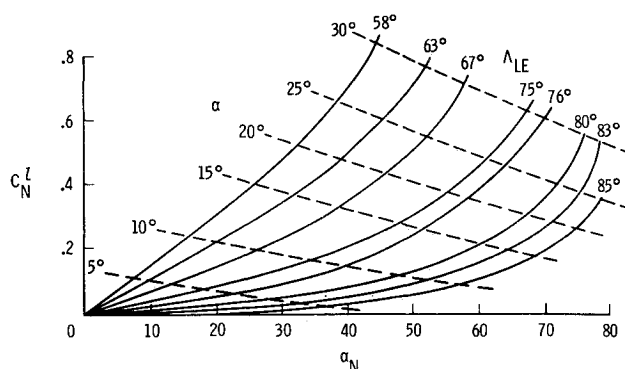


Fig. 9 Effect of Mach number, angle of attack, and leading-edge sweep on the lower-surface normal-force coefficient of flat delta wings.

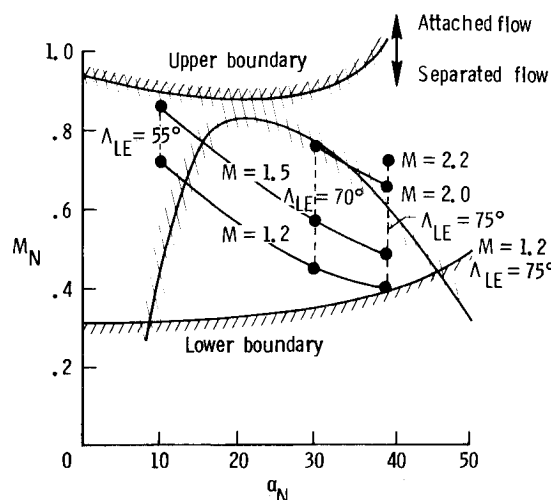


Fig. 10 Matrix of points for 0.4 design normal-force coefficient.

normal-force coefficient (C_N^l) is plotted as a function of the normal angle of attack (α_N) and results in a family of constant leading-edge sweep curves. Each of these curves is comprised of a range of Mach numbers, with the only limitation being that the normal Mach number (M_N) of all these data be less than 1.0. However, this correlation of the data did result in a variation with Mach number of approximately $\pm 0.01 C_N$ and, as a result, each curve represents the mean value. Also plotted in the figure for reference are lines of constant angle of attack. The data show that the lower surface produces a nonlinearly increasing normal-force increment with increasing angle of attack, and it can be seen that the nonlinearity increases with an increase in leading-edge sweep.

An evaluation of the data of Figs. 7 and 9 supports the findings previously observed in Fig. 2 which indicate that nonlinear lift is most pronounced for extremely highly swept wings at low Mach numbers. For these very low values of the parameter $\beta \cot \Lambda_{LE}$, the highly nonlinear character of the lower-surface normal-force coefficient will add to the linear character of the upper-surface normal-force coefficient and produce a total lift force which will increase in a nonlinear sense. Similarly, Figs. 7 and 9 can be used to show that the reduction in lift-curve slope with an increase in leading-edge sweep is primarily a lower-surface-dominated effect and the increase in lift-curve slope with a decrease in Mach number is an upper-surface-dominated effect.

Identification of a Separated-Flow Wing-Design Space

Imposing a design C_N value and requiring that the design C_N be distributed between the upper and lower wing surfaces such that the upper-surface normal-force coefficient will

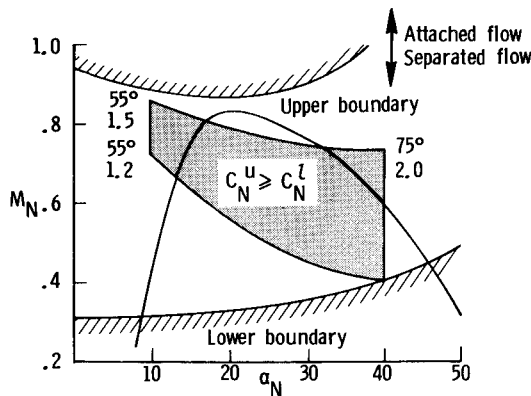


Fig. 11 Design space for 0.4 design normal-force coefficient.

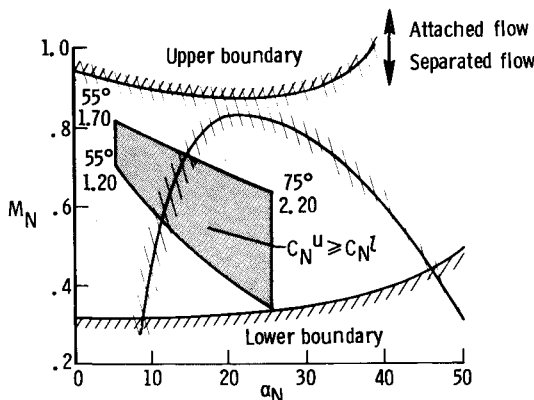


Fig. 12 Design space for 0.2 design normal-force coefficient.

always equal or exceed the lower-surface normal-force coefficient ($C_N^u \geq C_N^l$), the data presented in Figs. 7 and 9 can be used in an iterative sense to define the feasible high-lift separated-flow design space. Presented in Fig. 10 is a matrix of nine points, the solid circular symbols identified by their associated Mach number and leading-edge sweep values, that satisfies the distributive normal-force relationship ($C_N^u \geq C_N^l$) for a $C_N \approx 0.40$ design condition. Each of the points in the matrix was determined by iterating through Figs. 7 and 9 until the distributive requirement was satisfied. The matrix of feasible solutions presented in Fig. 10 can be thought of in terms of lines of constant Mach number (solid lines) in which both α and Λ_{LE} vary and lines of constant leading-edge sweep (dashed lines) in which only the Mach number varies. The boundaries of this particular design space are defined on the right by a leading-edge sweep of 75 deg, on the bottom by the minimum Mach number of 1.2, and on the left by a leading-edge sweep of 55 deg. Iterating through the design process the maximum Mach number for which a given geometry (leading-edge sweep) satisfies the distributive requirement is defined.

Presented in Figs. 11 and 12 are the design space for a design C_N value of 0.40 and 0.20, respectively. The graphs of Figs. 11 and 12 indicate that a reduction in the design C_N value expands the range of feasible solutions. The increased range of feasible Mach numbers for a decrease in design C_N results from a softening of the vacuum limit effect thus allowing the extension to higher Mach numbers. The apparent reduction in the size of the design space with reduced design C_N is strictly graphical in nature due to the nonlinearly decreasing relationship between α and α_N . In the process of deriving these correlations for flat, sharp leading-edge, delta wings, pressure data for nondelta planforms and cambered wings were reviewed selectively and showed that only slight variations in the magnitude and trends of the flat delta wing C_N^u , $C_{p,min}^u$ and C_N^l would be expected.

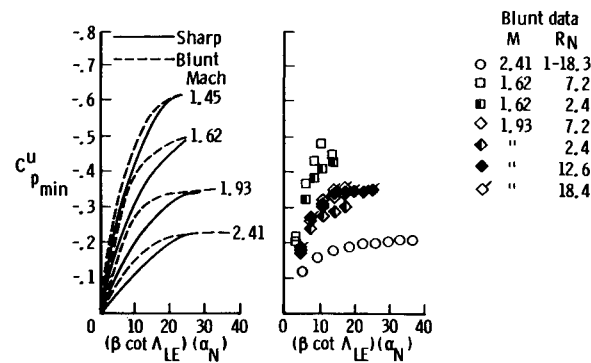


Fig. 13 Effect of leading-edge radius and Reynolds number on the minimum upper-surface pressure coefficient for flat delta wings.

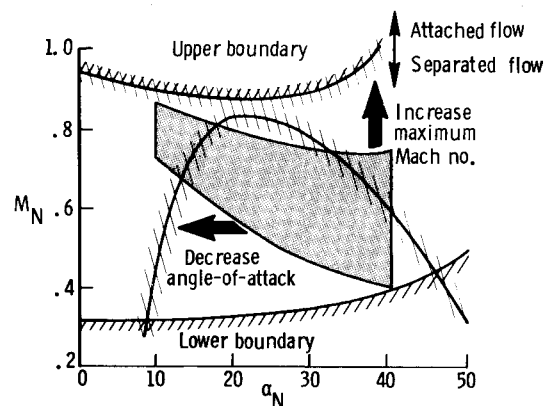


Fig. 14 Effect of leading-edge radius and Reynolds number on wing-design space.

Based upon existing pressure data for flat, sharp leading-edge, delta wings with M_N always less than 1.0, a series of graphs has been presented that will allow the designer to incorporate nonlinear lower- and upper-surface flow effects into the preliminary wing-design process. To extend these findings further, the effects associated with varying leading-edge bluntness and Reynolds number (R_N) are presented in Figs. 13-15. The data of Fig. 13 show the effect leading-edge bluntness and R_N has on the upper-surface minimum pressure value. The $C_{p,min}^u$ data are plotted as a function of the parameter $\alpha_N \beta \cot \Lambda_{LE}$ for flat wings at conditions in which the flow has separated at the leading edge. The data in the left portion of the figures show that leading-edge bluntness increases the minimum upper-surface pressure coefficient for a given value of $\alpha_N \beta \cot \Lambda_{LE}$, but does not affect the maximum level of $C_{p,min}^u$. The data in the right portion of the figure show that increasing R_N for a blunt leading edge, also increases the minimum upper-surface pressure coefficient for a given value of $\alpha_N \beta \cot \Lambda_{LE}$; however, these effects decrease with an increase in Mach number. The data of Fig. 13 can be used to show the shift in the wing-design space which would be expected in going from a sharp to a blunt leading edge (Fig. 14). The ability to attain a larger negative upper-surface pressure coefficient for a given angle of attack (see Fig. 13) would tend to increase the maximum design Mach number and also provide a given level of lift at a lower angle of attack. The result of lowering the required wing incidence to obtain a given level of lift is reflected in Fig. 15 where the value βC_{L_α} is plotted as a function of the parameter $\beta \cot \Lambda_{LE}$. The graph shows that for $\beta \cot \Lambda_{LE}$ values greater than 0.50, the addition of wing leading-edge bluntness increases the slope of the lift curve over that of a sharp leading-edge delta wing indicating that leading-edge bluntness could be an important design variable in separated-flow wing design.

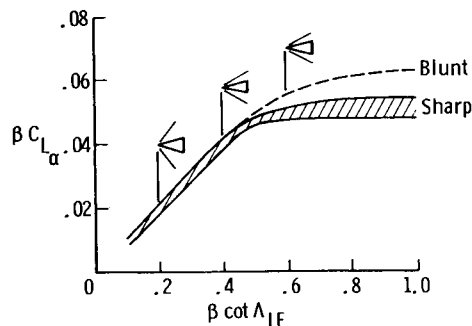


Fig. 15 Effect of leading-edge radius and Reynolds number of the lift-curve slope for flat delta wings.

The data presented in Figs. 4-9 showed that at supersonic speeds significant amounts of nonlinear flow exist on flat, sharp leading-edge, delta wings, and the data of Figs. 13-15 showed that the nonlinear characteristics of delta wings are affected by leading-edge bluntness and Reynolds number. These nonlinear characteristics which occur on both the upper and lower surfaces of a wing at high-lift conditions are summarized in Figs. 7 and 9 to provide a fundamental understanding to the designer.

Concluding Remarks

An investigation of the aerodynamics of sharp leading-edge delta wings at supersonic speeds has been conducted. The supporting experimental data for this investigation were taken from published force, pressure, and flow-visualization data in which the Mach number normal to the wing leading edge is always less than 1.0. The primary objective of this study was to determine the real-flow limitations associated with the high-lift, separated-flow, wing-design concepts, and to define a wing-design space applicable to separated flows at supersonic speeds.

By correlating the existing data for uncambered delta wings, it was shown that at supersonic speeds significant amounts of nonlinear flow exist on both the upper and lower surfaces. These individual upper- and lower-surface nonlinear normal-force characteristics were presented in the form of two charts. The upper-surface data showed that both the normal-force coefficient and minimum pressure coefficients increase nonlinearly with a decreasing slope with increasing angle of attack. In addition, the upper-surface minimum pressure coefficient data also showed that the percent of the vacuum pressure attainable is reduced with increasing Mach number such that at $M = 1.50$, 97% of vacuum was realized and at $M = 3.50$, only 75% of vacuum was achieved. The lower-surface normal-force coefficient was shown to be independent of Mach number and was found to increase nonlinearly with an increasing slope. The charts were used to define a wing-design space for sharp leading-edge delta wings. Additional analysis indicated that increasing leading-edge bluntness and Reynolds number will significantly affect the nonlinear upper-surface characteristics of delta wings.

References

- ¹Shapiro, A. H., *The Dynamics and Thermodynamics of Compressible Fluid Flow, Vols. I & II*, The Ronald Press Co. New York, 1954.
- ²Mayer, J. P., "A Limit Pressure Coefficient and an Estimation of Limit Forces on Airfoils at Supersonic Speeds," NACA RM-L8F23, Aug. 1948.
- ³Carlson, H. W. and Middleton, W. D., "A Numerical Method for the Design of Camber Surfaces of Supersonic Wings with Arbitrary Planforms," NASA TN D-2341, 1964.
- ⁴Carlson, H. W. and Miller, D. S., "Numerical Methods for the Design and Analysis of Wings at Supersonic Speeds," NASA TN D-7713, 1974.
- ⁵Carlson, H. W., "Aerodynamic Characteristics at Mach Numbers 2.05 of a Series of Highly-Swept Arrow Wings Employing Various Degrees of Twist and Camber," NASA TM X-332, 1960.
- ⁶Miller, D. S. and Schemensky, R. T., "Design Study Results of a Supersonic Cruise Fighter Wing," AIAA Paper 79-0062, Jan. 1979.
- ⁷Miller, D. S., Pittman, J. L., and Wood, R. M., "An overview of Non-Linear Supersonic Wing-Design Studies," AIAA Paper 83-0182, Jan. 1983.
- ⁸Lambourne, N. C. and Bryer, D. W., "Some Measurements in the Vortex Flow Generated by a Sharp Leading Edge Having 65 Degrees Sweep," ARC Tech. Rep., C.P. 477, 1960.
- ⁹Manno, M. E., "Transonic Pressure Measurements and Comparison of Theory to Experiment for Three Arrow-Wing Configurations. Vol. I: Experimental Data Report—Basic Data and Effect of Wing Shape," NASA CR-165701, Nov. 1979.
- ¹⁰Rao, D. M., "Leading-Edge Vortex Flaps for Enhanced Subsonic Aerodynamics of Slender Wings," ICAS 80-13.5, 1980.
- ¹¹Rao, D. M., "Segmented Vortex Flaps," AIAA Paper 83-0424, Jan. 1983.
- ¹²Boatright, W. B., "Experimental Study and Analysis of Loadings and Pressure Distributions on Delta Wings due to Thickness and to Angle of Attack at Supersonic Speeds," NACA RM-L56114, Dec. 1956.
- ¹³Hill, W. A. Jr., "Experimental Lift of Low-Aspect-Ratio Triangular Wings at Large Angles of Attack and Supersonic Speeds," NACA RM-A57117, Nov. 1957.
- ¹⁴Igglesden, M. S., "Wind Tunnel Measurements of the Lift-Dependent Drag of Thin Conically Cambered Delta Wings at Mach Numbers 1.4 and 1.8," RAE TN AERO. 2677, April 1960.
- ¹⁵Menees, G. P., "Lift, Drag, and Pitching Moment of an Aspect-Ratio-2 Triangular Wing with Leading-Edge Flaps Designed to Simulate Conical Camber," NASA Memo 10-5-58A, Dec. 1958.
- ¹⁶Ellis, M. C. Jr. and Hasel, L. E., "Preliminary Investigation at Supersonic Speeds of Triangular and Sweptback Wings," NACA TN-1955, Oct. 1949.
- ¹⁷Stallings, R. L. Jr. and Lamb, M., "Wing-Alone Aerodynamic Characteristics for High Angles of Attack at Supersonic Speeds," NASA TP-1889, July 1981.
- ¹⁸Brown, C. E. and Michael, W. H. Jr., "On Slender Delta Wings with Leading-Edge Separation," NACA TN-3430, April 1955.
- ¹⁹Katzen, E. D. and Pitts, W. C., "Load Distributions on Wings and Wing-Body Combinations at High Angles of Attack and Supersonic Speeds," NACA RM-A55E17, July 1955.
- ²⁰Hatch, J. E. Jr. and Gallagher, J. J., "Aerodynamic Characteristics of a 68.4 deg Delta Wing at Mach Numbers of 1.6 and 1.9 over a Wide Reynolds Number Range," NACA RM-L53108, Nov. 1953.
- ²¹Hatch, J. E. Jr., and Hargrave, L. K., "Effect of Reynolds Number of the Aerodynamic Characteristics of a Delta Wing at a Mach Number of 2.41," NACA RM-L51H06, Oct. 1951.
- ²²Michael, W. H. Jr., "Flow Studies on Flat-Plate Delta Wings at Supersonic Speed," NACA TN-3472, July 1955.
- ²³Michael, W. H. Jr., "Flow Studies on Drooped-Leading-Edge Delta Wings at Supersonic Speed," NACA TN-3614, Jan. 1956.
- ²⁴Boyd, J. W. and Phelps, E. R., "A Comparison of the Experimental and Theoretical Loading over Triangular Wings at Supersonic Speeds," NACA RM-A50J17, Jan. 1951.
- ²⁵Kaattari, G. E., "Pressure Distributions on Triangular and Rectangular Wings to High Angles of Attack—Mach Numbers 1.45 and 1.97," NACA RM-A54D19, June 1954.
- ²⁶Hall, C. F., "Lift, Drag, and Pitching Moment of Low-Aspect-Ratio Wings at Subsonic and Supersonic Speeds," NACA RM-A53A30, April 1953.
- ²⁷Squire, L. C., Jones, J. G., and Stanbrook, A., "An Experimental Investigation of the Characteristics of Some Plane and Cambered 65° Delta Wings at Mach Numbers from 0.7 to 2.0," ARC R&M 3305, 1963.
- ²⁸Larsson, P. O., "A Note on Supersonic and Transonic Flow Around Delta Wings," Seminar on Wind-Tunnel Technology and Aerodynamics, Royal Institute of Technology, Stockholm, Sweden, May 1954.
- ²⁹Briggs, M. M., Reed, R. E., and Nielsen, J. N., "Wing-Alone Aerodynamic Characteristics to High Angles of Attack at Subsonic and Transonic Speeds," Nielsen Engineering & Research, Inc., Mountain View, Calif. TR-269, Sept. 1982.
- ³⁰Vincenti, W. G., Nielsen, J. G., and Matteson, F. H., "Investigation of Wing Characteristics at a Mach Number of 1.53. I—Triangular Wings of Aspect Ratio 2," NACA RM-A7110, Dec. 1947.

³¹Love, E. S., "Investigations at Supersonic Speeds of 22 Triangular Wings Representing Two Airfoil Sections for Each at 11 Apex Angles," NACA Rept. 1238, 1955.

³²Bertram, M. H. and McCauley, W. D., "Investigation of the Aerodynamic Characteristics of High Supersonic Mach Numbers of a Family of Delta Wings Having Double-Wedge Sections with the Maximum Thickness at 0.18 Chord," NACA RM-L54G28, Oct. 1954.

³³Gallagher, J. J. and Mueller, J. N., "An Investigation of the Maximum Lift of Wings at Supersonic Speeds," NACA Rept. 1227, 1955.

³⁴Ulman, E. F. and Dunning, R. W., "Aerodynamic Characteristics of Two Delta Wings at Mach Number 4.04 and Correlations of Lift and Minimum-Drag Data for Delta Wings at Mach Numbers from 1.62 to 6.9," NACA RM-L52K19, 1952.

³⁵Squire, L. C., "Experimental Work on the Aerodynamics of Integrated Slender Wings for Supersonic Flight Progress," *Aerospace Sciences*, Vol. 20, 1980, pp. 1-96.

³⁶Kulfan, R. M., "Wing Geometry Effects on Leading Edge Vortices," AIAA Paper 79-1982, Aug. 1979.

³⁷Brown, C. E. and Michael, W. H., "Effect of Leading-Edge Separation on the Lift of a Delta Wing," *Journal of Aeronautical Sciences*, Vol. 21, No. 90, Oct. 1954, p. 690-694.

³⁸Squire, L. C., "Camber Effects on the Non-Linear Lift of Slender Wings with Sharp Leading Edges," ARC CP 924, 1967.

³⁹Miller, D. S. and Wood, R. M., "An Investigation of Wing Leading-Edge Vortices at Supersonic Speeds," AIAA Paper 83-1816, July 1983.

⁴⁰Stanbrook, A. and Squire, C. C., "Possible Types of Flow at Swept Leading Edges," *Aeronautics Quarterly*, Vol. XV, Feb. 1964, pp. 73-82.



The news you've been waiting for...

Off the ground in January 1985... |

Journal of Propulsion and Power

Editor-in-Chief
Gordon C. Oates
University of Washington

Vol. 1 (6 issues) 1985 ISSN 0748-4658
Approx. 96 pp./issue

Subscription rate: \$170 (\$174 for.)
AIAA members: \$24 (\$27 for.)

To order or to request a sample copy, write directly to AIAA,
Marketing Department J, 1633 Broadway, New York, NY
10019. Subscription rate includes shipping.

"This journal indeed comes at the right time to foster new developments and technical interests across a broad front."

—E. Tom Curran,

Chief Scientist, Air Force Aero-Propulsion Laboratory

Created in response to *your* professional demands for a **comprehensive, central publication** for current information on aerospace propulsion and power, this new bimonthly journal will publish **original articles** on advances in research and applications of the science and technology in the field.

Each issue will cover such critical topics as:

- Combustion and combustion processes, including erosive burning, spray combustion, diffusion and premixed flames, turbulent combustion, and combustion instability
- Airbreathing propulsion and fuels
- Rocket propulsion and propellants
- Power generation and conversion for aerospace vehicles
- Electric and laser propulsion
- CAD/CAM applied to propulsion devices and systems
- Propulsion test facilities
- Design, development and operation of liquid, solid and hybrid rockets and their components